сообщения
объединенного
института
ядерных
исследований
дубна

E14-85-576

J.Braziewicz, E.Braziewicz, G.M.Osetynski,
M.Pajek, J.Płoskonka, A.Purev

K-SHELL x-RAY CROSS SECTIONS OF SELECTED ELEMENTS FROM Ti TO Sb FOR INCIDENT PROTONS AND ^{4}He IONS

1985

Бразевич Я. и др. E14-85-576

Сечение выхода характеристического рентгеновского излучения K-оболочки для элементов от Ti до Sb при возбуждении их протонами и ионами ^{4}He

Измерялись сечения выхода характеристического рентгеновского излучения K-оболочки для тонких мишеней Ti, Se, Rb, Zr, Nb, Mo, Pd, Ag и Sb при протонном их возбуждении и для тонких мишеней Ti, Cr, Co, Se, Rb, Zr, Nb, Mo, Pd, Ag и Sn при возбуждении ионами ^{4}He при энергиях 1,5-3,8 МэВ. Из приведенных измерений рассчитаны сечения ионизации K-оболочки, которые сравнивались с теоретическими расчетами по теории ECPSSR, базирующейся на борновском приближении плоских волн (PWBA) с введением поправок на измерение энергии связи, поляризацию оболочек и релятивистский эффект для электронов атома мишени. Одновременно учитывалось влияние отклонения в кулоновском поле ядра, а также потери энергии для падающей частицы во время столкновения с атомом мишени. Приводится значение отношений K_{β}/K_{α}, которые сравниваются с данными других авторов и с теоретическими значениями.

Работа выполнена в Лаборатории нейтронной физики ОИЯИ.

Сообщение Объединенного института ядерных исследований. Дубна 1985

Braziewicz J. et al. E14-85-576

K-Shell x-Ray Cross Sections of Selected Elements from Ti to Sb for Incident Protons and ^{4}He Ions

The K-shell x-ray production cross sections and K_{β}/K_{α} ratios have been measured for thin targets of Ti,Se,Rb, Zr, Nb, Mo , Pd, Ag, Sb bombarded by protons and for thin targets of Ti, Cr, Co, Cu, Se, Rb, Zr, Nb, Mo, Pd, Ag, Sn bombarded by ^{4}He ions over energy range of 1.5-3.8 MeV. The ionisation cross sections were calculated using atomic K-shell fluorescence yields and compared with the plane-wave Born approximation (PWBA) modified to include the effects of increasing target electron binding energy, target electrons polarization, Coulomb deflection of incident projectile and energy-loss effect in ionisation process, resulting in the ECPSSR theory. The universal character of K-shell ionisation cross sections is discussed. The K_{β}/K_{α} ratios are compared with the theoretical predictions and with results reported by other authors.

The investigation has been performed at the Laboratory of Neutron Physics, JINR.

Communication of the Joint Institute for Nuclear Research. Dubna 1985

1. INTRODUCTION

Inner shell ionization in light-ion-atom collisions has long been studied from both theoretical and experimental points of view, but has received special attention in recent years. This is mainly due to the progress in experimental techniques and because of a large amount of reliable experimental data available to do comparison with existing theories. On the other hand, the knowledge of inner shell ionisation cross sections is necessary for resolving many analytical problems, for example by particle-induced x-ray emission (PIXE) method.

Considerable progress in description of ionisation process has been made since the development of basic theories: the plane-wave Born approximation (PWBA)[1], the semiclassical approximation (SCA)[2] and the binary encounter approximation (BEA)[3,4]. For light ion bombardment of heavier atoms direct Coulomb ionisation is the dominant mechanism of inner shell vacancy production and may be described successfully in terms of PWBA approximation with corrections for binding-polarization effect for target-atom electrons and for Coulomb deflection and energy-loss effects for incident particle, resulting in the ECPSSR theory of Brandt and Lapicki[5,6].

The experimental data for K-shell ionisation cross sections have been summarized by Gardner and Gray[7] and, lately, compared extensively with the ECPSSR theory (including recent experimental results) by Paul[8,9], where agreement within 6% was found between average K-shell data and theory.

This paper reports on the results of the K-shell x-ray production cross sections due to bombardment of this targets of Ti, Se, Rb, Zr, Nb, Mo, Pd, Ag, and Sb by protons and thin targets of Ti, Cr, Co, Cu, Se, Rb, Zr, Nb, Mo, Pd, Ag, and Sn by ^{4}He ions in the energy range 1.5-3.8 MeV. We compare present results with predictions of the ECPSSR theory. The values of K_β/K_α ratios are reported and compared with the theoretical values of Scofield[10] and with other experimental data.

2. EXPERIMENTAL SET-UP

Proton and ^{4}He ion beams of 1.5-3.8 MeV energy have been used from Van de Graaf accelerator at the Laboratory of Neutron Physics of the Joint Institute for Nuclear Research at Dubna. The experimental apparatus has been described in detail earlier[11]. The beam was formed by a set of four graphite collimators and a pair of sweeping plates, so we obtained a uniform beam spot of 2 mm diameter at the target. The targets were positioned at 45° to the beam axis and were mounted on a multiple target holder. Around the target holder a graphite cylinder at potential of -600 V was placed to suppress secondary electrons from the target. Beam currents were monitored by charge collection on the target and on the Faraday cup. The Si(Li) detector with an energy resolution of 220 eV at 6.4 keV of ^{57}Co source was placed outside the chamber at 90° relative to beam direction. The x-rays emitted from targets passed through the 10 μm thick metallised mylar window of the chamber, a 5 mm air gap and a 25 μm thick beryllium detector window before reaching the detector.

The total efficiency of the x-ray detector, consisting in the intrinsic efficiency of the Si(Li) detector, the relative detector solid angle and x-ray attenuation factor for absorption between target and intrinsic region of detector, was determined from measurements of the K-x rays emitted from the calibrating targets. The calibration was performed using the thin targets of fourteen elements from Al to Sn (K-x ray energies from 1.5 to 30 keV) and protons with energy of 2-3 MeV. For these elements the x-ray production cross sections were taken from fitted cross section - atomic number dependences using existing K-shell experimental data[7] for energies of interest. Additionally, the radioisotopic ^{57}Co and ^{241}Am calibrating sources were used.

To suppress low-energy x-rays mylar filters of thicknesses from 100 to 400 μm or 230 μm silicon filter were put into air gap between the windows of chamber and detector. A pile-up rejector was associated with the amplifier and dead-time corrections for counting electronics were made.

The elements to be studied were vacuum evaporated onto 0.2 mm silicon backing using standard evaporation technique. The thicknesses of targets were measured by 2-3 MeV ^{4}He ions backscattered into the silicon surface-barrier detector positioned at 135° to the beam axis. The measured elements and their thicknesses are listed in Table 1.

3. DATA ANALYSIS

The spectra for studied elements (Table 1) were analysed on the PDP-11/70 computer to remove the background and resolve the partial transitions (K_α and K_β). The x-ray spectrum accumulation times were selected in such a manner that areas under K_β peaks were greater than 10^3. Experimental x-ray production cross sections for K_α and K_β lines were determined as a function of proton or ^{4}He ion energy from the following relationship:

$$\overline{\sigma^x_{k_i}} = \frac{N_{k_i}}{N_p N_T \epsilon_{tot}(k_i)}, \qquad (1)$$

where N_{k_i} is the dead-time corrected peak area, N_p is a number of incident ions determined from beam integration, N_T is a number of target atoms per square centimetre obtained from measurement of backscattered ^{4}He ions. The $\epsilon_{tot}(k_i)$ denotes the total detection efficiency for k_i line. The uncertainties in measured cross sections come from the following sources: peak area determination, target thickness, beam current integration and total detection efficiency. The value of partial and total uncertainties are listed in Table 2.

To reduce the uncertainties in cross sections connected with the projectile energy loss and x-ray absorption in the target the appropriate correction for cross sections was made as follows:

$$\sigma^x_{k_i} = \overline{\sigma^x_{k_i}} \left[1 - \frac{1}{2}(a_k - b)\frac{\Delta E}{E_0} - \frac{1}{2}\mu_{k_i}\Delta x\right]^{-1}, \qquad (2)$$

where $\sigma^x_{k_i}$ and $\overline{\sigma^x_{k_i}}$ are corrected and uncorrected cross sections ($i = \alpha, \beta$), respectively, and μ_{k_i} is the x-ray mass attenuation coefficient. This formula was obtained under assumption that the projectile energy loss ΔE in a target of thickness Δx is small relative to initial projectile energy E_0, and x-ray pro-

Table 1

Thicknesses of targets used in the measurement of K-shell x-ray production cross sections

Target	Thickness, μgcm^{-2}	Target	Thickness, μgcm^{-2}
^{22}Ti	31.8	^{41}Nb	17.0
^{24}Cr	63.1	^{42}Mo	9.5
^{27}Co	27.3	^{46}Pd	24.4
^{29}Cu	6.2	^{47}Ag	20.0
^{34}Se	45.1	^{50}Sn	11.5
^{37}Rb	10.2	^{51}Sb	66.2
^{40}Zr	7.2		

Table 2

Sources of uncertainties in measured cross sections

Sources	Range
Counting statistics of K_α and K_β x-ray yields	1-3%
Current integration	1.5%
Target thickness	4%
Detection efficiency	7%
Beam energy	1%
x-ray production cross sections[a)]	9%
Fluorescence yields[b)] ($22 \le Z_2 \le 51$)	5-2%
Ionisation cross sections[a)]	11-10%

a) Total uncertainty is the square root of sum of individual uncertainties.

b) According to Krause/13/

duction cross section and projectile stopping power S(E) varies near E_0 as E^{a_k} and E^b, respectively. The a_k and b parameters were derived by fitting a straight line to $\log\sigma(E)$ and $\log S(E)$ against $\log E$ near all energies of interest using theoretical ECPSSR/5,6/ values of x-ray production cross sections for each line and the tables of Williamson et al./12/ for proton and ^{4}He ion stopping power, respectively. In our case the value of this correction was less than 3%.

4. RESULTS AND DISCUSSION

The x-ray spectra for Ti, Se, Rb, Zr, Nb, Mo, Pd, Ag, and Sb were measured for proton energies of 1.46, 2.05, 2.50, 2.99, 3.20, 3.53, 3.60, 3.70, and 3.80 MeV and for Ti, Cr, Co, Cu, Se, Rb, Zr, Nb, Mo, Pd, Ag, and Sn for ^{4}He ion energies of 1.50, 2.01, 2.48, 2.99, 3.20, 3.49, 3.60, 3.70, and 3.80 MeV. The K-shell x-ray production cross sections were determined from measurements, as a sum of K_α and K_β transitions, and then were converted to ionisation cross sections σ_K^{exp} using the K-

Table 3

K-shell x-ray production cross sections. The energies are given in MeV and the cross sections are given in barns. The integers in parentheses indicate power of 10

Z_2	E_p	$\sigma_K^x(p)$	$E_{^4He}$	$\sigma_K^x(^4He)$	K_β/K_α
	1.46	8.99 (1)	1.50	4.71	0.130[a]
	2.05	2.14 (2)	2.01	1.89 (1)	
$_{22}$Ti	2.50	2.86 (2)	2.48	3.26 (1)	0.127[b]
	2.99	3.65 (2)	2.99	5.59 (1)	
	3.53	4.41 (2)	3.49	9.05 (1)	
		-	1.50	4.17	
		-	2.01	1.07 (1)	
$_{24}$Cr		-	2.48	2.31 (1)	0.121[b]
		-	2.99	4.11 (1)	
		-	3.49	6.91 (1)	
		-	1.50	1.16	
		-	2.01	3.28	
		-	2.48	6.75	0.134[b]
$_{27}$Co		-	2.99	1.23 (1)	
		-	3.20	1.55 (1)	
		-	3.49	1.99 (1)	
		-	1.50	9.60 (-1)	
		-	2.01	3.15	
$_{29}$Cu		-	2.48	6.55	0.136[b]
		-	2.99	1.23 (1)	
		-	3.49	2.03 (1)	
	1.46	4.85	1.50	1.33 (-1)	
	2.05	-	2.01	3.97 (-1)	
	2.50	1.46 (1)	2.48	8.30 (-1)	0.160[a]
	2.99	2.36 (1)	2.99	1.57	
$_{34}$Se	3.20	2.69 (1)	3.20	2.00	0.156[b]
	3.53	3.04 (1)	3.49	2.68	
	3.60	-	3.60	2.86	
	3.70	3.59 (1)	3.70	3.05	
	1.46	2.67	1.50	5.50 (-2)	0.183[a]
	2.05	7.41	2.01	1.85 (-1)	
$_{37}$Rb	2.50	1.23 (1)	2.48	4.10 (-1)	0.178[b]
	2.99	1.89 (1)	2.99	8.20 (-1)	
	3.53	2.45 (1)	3.49	1.48	
	1.46	1.15	1.50	2.20 (-2)	0.194[a]
	2.05	3.20	2.01	8.20 (-2)	
$_{40}$Zr	2.50	5.39	2.48	1.90 (-1)	0.196[b]
	2.99	8.67	2.99	3.67 (-1)	
	3.53	1.14 (1)	3.49	6.40 (-1)	

Table 3 (continued)

Z_2	E_p	$\sigma_K^x(p)$	$E_{^4He}$	$\sigma_K^x(^4He)$	K_β/K_α
	1.46	9.40 (-1)		-	
	2.05	2.59	2.01	6.20 (-2)	0.201[a]
	2.50	4.50	2.48	1.46 (-1)	
$_{41}$Nb	2.99	7.18	2.99	3.00 (-1)	0.200[b]
	3.53	1.04 (1)	3.49	5.03 (-1)	
	1.46	7.10 (-1)		-	
	2.05	1.97	2.01	4.90 (-2)	
	2.50	3.40	2.48	1.13 (-1)	0.206[a]
$_{42}$Mo	2.99	5.55	2.99	2.32 (-1)	
	3.53	-	3.49	4.00 (-1)	0.204[b]
	3.80	-	3.80	5.50 (-1)	
	1.46	3.00 (-1)	1.50	4.00 (-3)	
	2.05	8.60 (-1)	2.01	2.00 (-2)	
	2.50	1.70	2.48	5.00 (-1)	
	2.99	2.43	2.99	1.04 (-1)	
$_{46}$Pd	3.20	-	3.20	1.35 (-1)	
	3.53	4.11	3.49	1.91 (-1)	
	3.60	4.46	3.60	2.11 (-1)	
	3.70	4.51		-	
	1.46	2.63 (-1)	1.50	2.70 (-3)	
	2.05	6.68 (-1)	2.01	1.90 (-2)	
	2.50	1.21	2.48	3.90 (-2)	
	2.99	1.95	2.99	8.20 (-2)	0.226[a]
$_{47}$Ag	3.20	2.44	3.20	1.13 (-1)	
	3.53	3.06	3.49	1.43 (-1)	
	3.60	-	3.60	1.65 (-1)	
	3.70	3.57	3.70 (-1)	1.86 (-1)	
		-	2.48	1.90 (-2)	
		-	2.99	3.90 (-2)	
$_{50}$Sn		-	3.49	7.20 (-2)	
	2.05	3.15 (-1)		-	
$_{51}$Sb	2.50	6.06 (-1)		-	
	2.99	9.55 (-1)		-	
	3.20	1.32		-	

a) K_β/K_α ratio for proton bombardment.
b) K_β/K_α ratio for ^{4}He bombardment.

shell fluorescence yields of Krause /13/. The values of ionisation cross sections obtained in this way were used to compare with the ECPSSR theory. Present results concerning x-ray production cross sections are listed in Table 3.

The K-shell ionisation cross sections in the ECPSSR theory can be written, according to Brandt and Lapicki /6/, as:

$$\sigma_K^{ECPSSR} = 9E_{10}\left[\frac{2\pi d q_{0K}\zeta_K}{Z_K(Z_K+1)}\right] f_K(z_K)\,\frac{\sigma_{0K}}{\zeta_K\Theta_K}\,F_K(\xi_K^R/\zeta_K,\ \zeta_K\Theta_K) \qquad (3)$$

with $\sigma_{0K}=8\pi a_0^2 Z_1^2/Z_{2K}^4$, where a_0 is Bohr radius and $Z_{2K}=Z_2-0.3$, with Z_1 and Z_2 being projectile and target atomic numbers, respectively. Here $\Theta_K=E_K/Z_{2K}^2R$ denotes reduced binding energy (E_K) of electron, where R is Rydberg constant. The variable ξ_K^R is reduced collision-valocity parameter $\xi_K=2v_1/Z_{2K}v_0\Theta_K$ corrected for relativistic effect ($\xi_K^R=[m_K^R]^{1/2}\xi_K$), with relativistic correction factor m_K^R from /5/), where v_1 is projectile velocity and v_0 denotes Bohr velocity. The form of scaling parameter ζ_K, describing the binding-polarization effect, is given by Basbas /14/. The energy-loss effect is accounted in terms of $Z_K=(1-\zeta_K\Delta_K)^{1/2}$ quantity, with Δ_K being minimum fractional energy-loss of projectile during K-shell ionisation (in the center-of-mass system), by analytical function $f_K(Z_K)$ given by Brandt and Lapicki /6/. The Coulomb deflection of a projectile /14/ is taken into account in Eq.(3) via an exponential integral of the order of ten, E_{10}, where q_{0K} is the minimum momentum transfer and d is one-half distance of closest approach in head-on collision. The $F_K(\xi_K,\Theta_K)$ function was tabulated by Rice et al. /15/. However, in the case of ECPSSR theory, the values of this function must be taken for scaled ξ_K^R/ζ_K and $\zeta_K\Theta_K$ variables.

For the K-shell, when $\xi_K<1$, $F_K(\xi_K,\Theta_K)$ starts to be universal in ξ_K. i.e., independent of Θ_K and $F_K^{univ}(\xi_K)$ can be calculated by formula of Brandt et al. /16/:

$$F_K^{univ}(\xi_K) = \frac{2^9}{45}\,\xi_K^8(1+1.72\,\xi_K^2)^{-4}. \qquad (4)$$

To look for universal character of measured ionisation cross sections the experimentally derived K-shell ionisation cross sections were transferred to experimental $F_K^{exp}(\xi_K)$ function defined as follows:

$$F_K^{exp}(\xi_K) = \frac{\sigma_K^{exp}}{\sigma_{0K}}\cdot\frac{\zeta_K\Theta_K}{9E_{10}\left[\frac{2\pi d q_{0K}\zeta_K}{Z_K(Z_K+1)}\right] f_K(Z_K)}. \qquad (5)$$

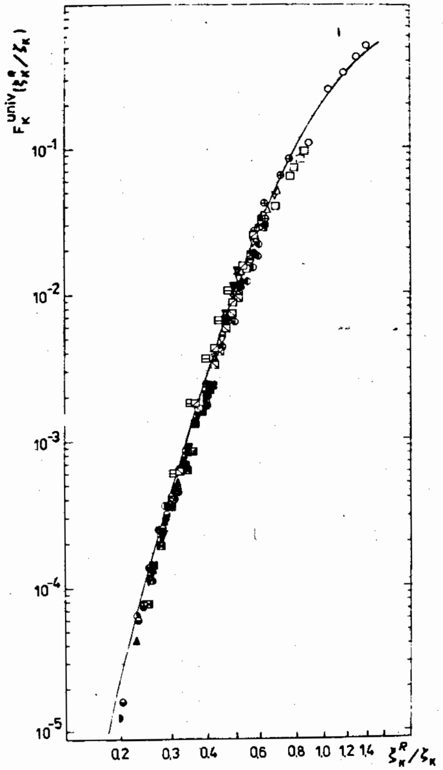

Fig.1. Comparison of experimental and theoretical (solid curve) values of universal function F_K^{univ} *(eq.(4)) according to the ECPSSR theory versus scaled velocity parameter* ξ_K^R/ζ_K. *The experimental points were derived from measured* K*-shell ionisation cross sections using Eq.(5)) and are marked as follows:* Ti *:* o – p *,* ● – ^{4}He*;* Cr *:* ⊠ – ^{4}He*;* Co *:* ⧅ – ^{4}He*;* Cu *:* ⊟ – ^{4}He*;* Se *:* □ – p*;* ■ – ^{4}He*;* Rb *:* ⊕ – p*,* ◉ – ^{4}He*;* Zr *:* Δ – p*,* ▲ – ^{4}He*;* Nb *:* ∇ – p*,* ▼ – ^{4}He*;* Mo *:* ⊠ – p *,* ◘ – ^{4}He *;* Pd *:* ⊖ – p*,* ⊖ – ^{4}He*;* Ag *:* ◐ – p*,* ◑ – ^{4}He*;* Sn *:* ⊖ – ^{4}He*;* Sb *:* ⧗ – p .

The values of this function are presented and compared with the universal function F_K^{univ} (Eq.(4)) on Fig.1, where universal nature of experimental data is evident over the range of ξ_K^R/ζ_K parameter of interest. Additionally, for estimation of residual nonuniversality of theoretical description, we have compared the results of universal function F_K^{univ} with nonuniversal one, F_K, for elements and energies of interest. On Fig.2 we present the relative deviation of universal function from nonuniversal one, $F_K/F_K^{univ}-1$, where deviation less than 6% was found for the case of proton impact for elements and energies studied. For ^{4}He ion excitation analogous relative deviation was less than for the case of proton.

In Fig.3 we present the experimentally obtained K_β/K_α ratios together with other experimental data and theoretical predictions of Scofield [10]. As can be seen from Fig.3 the ratios K_β/K_α measured by many authors agree within 20%. Uncertainties of our experimental data were estimated as 10% and were caused mainly by detector efficiency uncertainties. The K_β/K_α ratios were observed to be constant for a given element over the proton and ^{4}He ion energy of interest and are listed in Table 3.

In conclusion, the K-shell x-ray production cross sections by protons and ^{4}He ions have been measured for selected elements from Ti to Sb in energy range of 1.5 to 3.8 MeV. It has been shown, that measured K-shell ionisation cross sections can

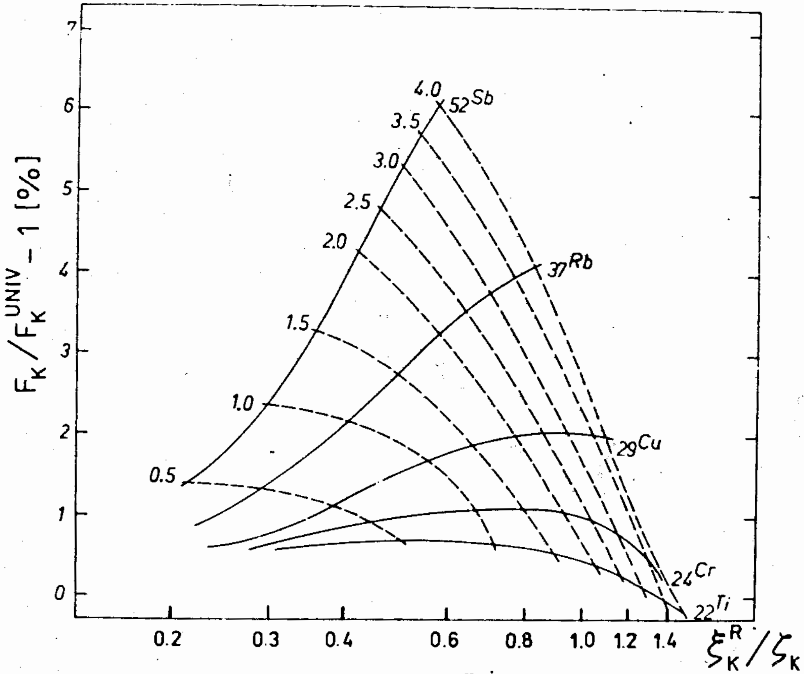

Fig.2. Relative deviation, $F_K/F_K^{univ}-1$, *of nonuniversal function* F_K *(see Eq.(3)) from universal one,* F_K^{univ} *(Eq.(44)), versus scaled velocity parameter for protons. The solid curves represent deviation for marked elements, while the dashed ones, for the ion energy given (in MeV).*

be reproduced by the ECPSSR theory supplied with universal F_K^{univ} function. The residual nonuniversal effects in theoretical approach were estimated to be less than 6% for both protons and ^{4}He ions for studied elements.

ACKNOWLEDGEMENTS

We wish to thank the staff of the Laboratory of Neutron Physics Van de Graaf generator for good work throught the time of this experiment.

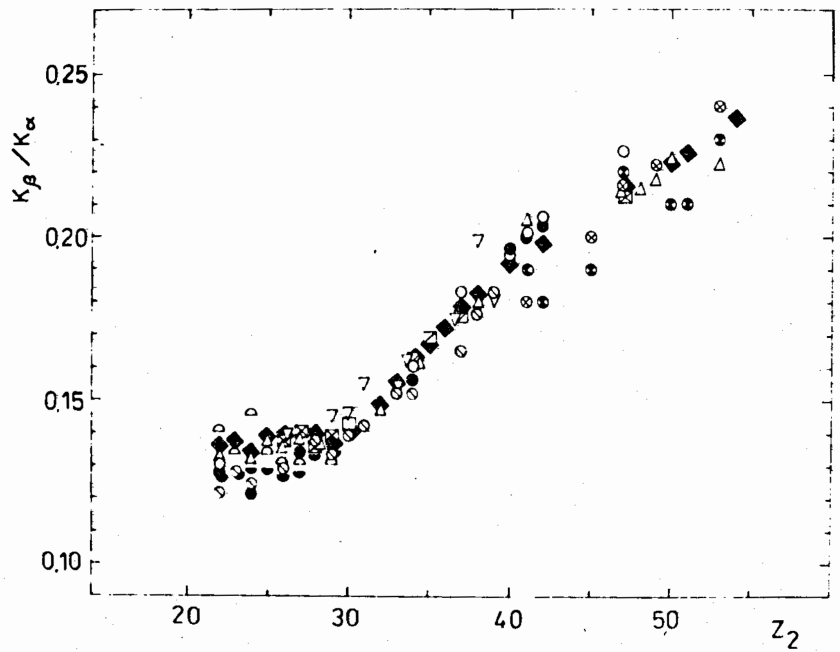

Fig.3. Experimentally determined K_β/K_α *ratios versus atomic number* Z_2 . o – p , ● – ^{4}He – *present experiment;* □ – p – *Tawara et al.*/17/: ⊡ – p – *Criswell and Gray*/18/: ⊗ – p , ⊗ – ^{4}He – *Wilson et al.*/19/; ∇ – p – *Lear and Gray*/20/; Δ – p – *Bonani et al.*/21/; ⌓ – p , ● – ^{4}He – *Bodard et al.*/22/; ⊠ – p – *Akselsson and Johansson*/23/: ⊘ – p – *McDaniel et al.*/24/; ♦ – *theoretical values of Scofield*/10/.

REFERENCES

1. Merzbacher E., Lewis H.W. Encyclopedia of Physics. Springer-Verlag, 1958, vol.34, p.166.
2. Bang J., Hansteen J.M. Kgl.Dan.Vid.Selsk.Mat.-Fys.Medd., 1959, vol.31, No.13.
3. Garcia J.D. Phys.Rev., 1970, A1, p.280.
4. Hansen J.S. Phys.Rev., 1973, A8, p.822.
5. Brandt W., Lapicki G. Phys.Rev., 1979, A20, p.465.
6. Brandt W., Lapicki G. Phys.Rev., 1981, A23, p.1717.
7. Gardner R.K., Gray T.J. At.Data Nucl.Data Tables, 1978, 21, p.515.
8. Paul H., Obermann W. Nucl.Instr.and Meth., 1983, 214, p.15.
9. Paul H. Nucl.Instr. and Meth., 1984, B4, p.211.
10. Scofield J.H. Phys.Rev., 1974, A9, p.1041.

11. Braziewicz E. et al. JINR, 18-81-503, Dubna, 1981.
12. Williamson C.F. et al. Rapport du Comisariat a l`Energie Atomique, CER-R 3042, France.
13. Krause M.O. J.Phys.Chem.Ref.Data, 1979, 8, p.307.
14. Basbas G. et al. Phys.Rev., 1978, A17, p.1655.
15. Rice R. et al. At.Data Nucl.Data Tables, 1977, 20, p.503.
16. Brandt W. et al. Phys.Rev.Lett., 1973, 30, p.351.
17. Tawara H. et al. Phys.Rev., 1974, A9, p.1617.
18. Criswell T.L., Gray T.J. Phys.Rev., 1974, A10, p.1146.
19. Wilson S.R. et al. Phys.Rev., 1977, A16, p.903.
20. Lear R., Gray T.J. Phys.Rev., 1973, A8, p.2469.
21. Bonani G. et al. Helvetica Phys.Acta, 1978, 51, p.272.
22. Bodart F. et al. X-Ray Spectrom., 1975, 4, p.161.
23. Akselsson R., Johansson T.B. Z.Phys., 1974, 266, p.245.
24. McDaniel F.D. et al. Phys.Rev., 1975, A11, p.1607.

Received by Publishing Department
on July 30, 1985.